applied optics

Influence of source parameters and atmospheric turbulence on the polarization properties of partially coherent electromagnetic vortex beams

Jiao Wang,[1,4] Xizheng Ke,[1,2,3,*] and Mingjun Wang[1]

[1]Faculty of Automation & Information Engineering, Xi'an University of Technology, Xi'an 710048, China
[2]Faculty of Physics and Telecommunications Engineering, Shaanxi University of Technology, HanZhong 723003, China
[3]Shaanxi Civil-Military Integration Key Laboratory of Intelligence Collaborative Networks, Xi'an 710126, China
[4]e-mail: jiaolun216@163.com
*Corresponding author: xzke@xaut.edu.cn

Received 27 February 2019; revised 4 June 2019; accepted 5 June 2019; posted 15 July 2019 (Doc. ID 361082); published 13 August 2019

In this paper, we introduce a vortex class of a partially coherent source of Schell type with an electromagnetic Gaussian Schell-model vortex (EGSMV) beam, which is the product of the partially coherent EGSM beam passing through a spiral phase modulator. The analytical expressions for the degree of polarization (DoP) and orientation angle of polarization (OAoP) of the EGSMV beam propagating through atmospheric turbulence are derived. The expressions are used to analyze the influence of topological charge, wavelength, and atmospheric turbulence on the DoP and OAoP of the EGSMV beam, and we come to some new conclusions. The larger the topological charge is, the bigger the dark spot in the center of the partially coherent EGSMV beam, the more dispersed the DoP distribution, and the wider the OAoP distribution are; therefore, there is more information received by the detector when the partially coherent EGSMV beam propagates in atmospheric turbulence. The longer the wavelength is, the smaller the near-surface refractive index structure constant and the larger the inner scale are and the more concentrated the DoP distribution is, but the influence of the outer scale is negligible. The number of petals, which is the shape of the OAoP distribution, is equal to just twice the topological charge. These results provide a theoretical basis for better control of coherent detection in optical communication when the partially coherent EGSMV beam propagating through atmospheric turbulence is used as the local oscillator in a wireless optical communication system.

https://doi.org/10.1364/AO.58.006486

1. INTRODUCTION

The state of polarization of the electromagnetic field is one of the most fundamental properties that describe the vector characteristics of the field and has attracted much attention because of its important potential applications in polarization control, free-space optical communications, particle trapping, target detection and recognition, etc., [1–3]. In the earlier period of the 1990s, Wu *et al.* pointed out that partially coherent beams are more resistant to turbulence than their fully coherent counterparts [4,5], and based on the unified theory of coherence and polarization [6–8], the polarization properties of partially coherent beams in random media have become a research hotspot. Eyyuboglu *et al.* used the coherent and polarization matrix to analyze the variation of degree of polarization (DoP) of a partially coherent beam with the propagation distance under different light source parameters [9]. Lin and Zheng *et al.* investigate the degree of coherence, the degree of polarization, the mean-squared beam width, and the degree of cross polarization of the partially coherent radially polarized beam in atmospheric turbulence [10,11]. Basso *et al.* suggest a method to access the second-order and Stokes parameters of a partially coherent and partially polarized Gaussian model optical field from an intensity interferometry experiment [12].

Furthermore, it is well known that a vortex beam with a spiral phase, described by a phase factor $\exp(-il\theta)$ with a topological charge l and azimuthal angle θ, carry an orbital angular momentum (OAM) equivalent to $l\hbar$ per photon [13], and the propagation properties of various types of scalar and electromagnetic vortex beams in atmospheric turbulence are an important area of study [14–18]. Ou *et al.* used the extended Huygens–Fresnel principle to derive the expressions of average intensity and DoP of the elliptically polarized vortex beam [16] in atmospheric turbulence. Luo *et al.* analyzed the degree of cross polarization of a stochastic electromagnetic vortex beam [17] and suggested a method to access the measurement of the OAM of the vector vortex beam, which is that the number of bright ring dislocations is equal to the topological charge of the vortex beam. Li *et al.* presented the effects of media on intensity, phase, and polarization of a vector Bessel vortex beam [18] through multilayered isotropic media. In addition to this, there are some types of vector vortex beams, such as higher-order radially polarized Laguerre–Gaussian beams [19], superposed vector Laguerre–Gaussian beams [20–22], radially polarized multi-cosine Gaussian correlated Schell-model beams [23,24], vector-vortex Bessel–Gauss beams [25], elliptical vortex beams [26], four-petal elliptic Gaussian vortex beams [27,28], and so on.

Combining the advantages of partially coherent beams and the special properties of vortex beams, in this study, we introduce a vortex class of partially coherent sources of Schell type with electromagnetic Gaussian Schell-model vortex (EGSMV) beam, which is the product of the partially coherent EGSM beam passing through a spiral phase modulator. Since the polarization control in wireless optical communication systems is an indispensable module, if the polarization states of the signal light and the local oscillator are inconsistent, it will directly affect the receiving sensitivity of the entire system. Therefore, we use the unified theory of coherence and polarization to derive the expressions for the DoP and orientation angle of polarization (OAoP) and analyze the influence of source parameters and atmospheric turbulence on the polarization properties of partially coherent EGSMV beams.

2. THEORETICAL FORMULATION

A. Propagation Properties

Based on the unified theory of coherence and polarization [7], a beam is generated by a source located in the $z = 0$ plane (the source plane) and propagates close to the positive z axis into the half-space $z > 0$. The cross-spectral density matrix (CSDM) can be given by [6]

$$\overleftrightarrow{W}(\boldsymbol{\rho}_1,\boldsymbol{\rho}_2;z) \equiv W_{ij}(\boldsymbol{\rho}_1,\boldsymbol{\rho}_2;z) = \begin{bmatrix} W_{xx}(\boldsymbol{\rho}_1,\boldsymbol{\rho}_2;z) & W_{xy}(\boldsymbol{\rho}_1,\boldsymbol{\rho}_2;z) \\ W_{yx}(\boldsymbol{\rho}_1,\boldsymbol{\rho}_2;z) & W_{yy}(\boldsymbol{\rho}_1,\boldsymbol{\rho}_2;z) \end{bmatrix}, \tag{1}$$

where $W_{ij}(\boldsymbol{\rho}_1,\boldsymbol{\rho}_2;z) = \langle E_i(\boldsymbol{\rho}_1;z)E_j^*(\boldsymbol{\rho}_2;z)\rangle$ and $(i,j = x,y)$. E_i and E_j are, respectively, the components of the random optical field in the x and y directions, and the asterisk represents the complex conjugate. $\boldsymbol{\rho}_1 = (\rho_1,\varphi_1)$ and $\boldsymbol{\rho}_2 = (\rho_2,\varphi_2)$ denote a pair of points with arbitrary transverse position vectors in the receiver plane at $z > 0$, and $\langle\rangle$ denotes the ensemble average.

The spatial coherence correlation statistical properties of a partially coherent beam at a pair of points with arbitrary transverse position vectors $\mathbf{r}_1 = (r_1,\theta_1)$ and $\mathbf{r}_2 = (r_2,\theta_2)$ in the source plane can be characterized by the CSDM. The CSDM of the EGSM beam at the source plane can be expressed in cylindrical coordinates as [29]

$$W_{ij}(\mathbf{r}_1,\mathbf{r}_2;0) = A_iA_j \exp\left[-\left(\frac{\mathbf{r}_1^2}{4w_{0i}^2}+\frac{\mathbf{r}_2^2}{4w_{0j}^2}\right)\right]\mu_{ij}(\mathbf{r}_1-\mathbf{r}_2), \tag{2}$$

where A_i and A_j are the amplitudes of the EGSM beam in the x and y directions. w_{0i} and w_{0j} are the beam radii of the Gaussian beam at the waist in the x and y directions; $\mu_{ij}(\mathbf{r}_1-\mathbf{r}_2)$ is the spectral degree of coherence at points $\mathbf{r}_1$ and $\mathbf{r}_2$ in the source plane and takes the following form:

$$\mu_{ij}(\mathbf{r}_1-\mathbf{r}_2) = B_{ij}\exp\left(-\frac{|\mathbf{r}_1-\mathbf{r}_2|^2}{2\delta_{ij}^2}\right), \tag{3}$$

where δ_{ij} is the coherence length of the source, and $\delta_{ij} = \delta_{ji}$. The parameters relating to spatial variation should meet the following set of conditions [30]:

$$B_{ij} = 1 \;\; i = j; \quad |B_{ij}| \le 1 \;\; i \ne j; \quad B_{ij} = B_{ji}^*, \tag{4a}$$

$$\max\{\delta_{ii},\delta_{jj}\} \le \delta_{ij} \le \min\{\delta_{ii}/|B_{ij}|^{0.5},\delta_{jj}/|B_{ij}|^{0.5}\}. \tag{4b}$$

If the partially coherent EGSM beam passes through a spiral phase modulator with modulation transfer function $\exp(-il\theta)$, where l is the azimuth index (also called the topological charge) and θ is the azimuth angle in cylindrical coordinates, the partially coherent EGSMV beam will carry a spiral phase, and its CSDM can be expressed as

$$W_{ij}(\mathbf{r}_1,\mathbf{r}_2;0) = A_iA_jB_{ij}\exp\left[-\left(\frac{\mathbf{r}_1^2}{4w_{0i}^2}+\frac{\mathbf{r}_2^2}{4w_{0j}^2}\right)\right] \times \exp\left(-\frac{|\mathbf{r}_1-\mathbf{r}_2|^2}{2\delta_{ij}^2}\right)\exp[-il(\theta_1-\theta_2)]. \tag{5}$$

Equation (5) is obtained by modulating the phase of the partially coherent EGSM beam without affecting the degree of coherence of the partially coherent EGSMV beam. Therefore, the expression of the degree of coherence of the partially coherent EGSMV beam is still Eq. (3).

According to the extended Huygens–Fresnel principle [31], when the partially coherent EGSMV beam propagates from the source plane ($z = 0$) to the receiver plane ($z > 0$) in atmospheric turbulence, the elements of the CSDM can be expressed by

$$\begin{aligned} W_{ij}(\boldsymbol{\rho}_1,\boldsymbol{\rho}_2;z) = {} & A_iA_jB_{ij}\left(\frac{k}{2\pi z}\right)^2 \iint \exp\left[-\left(\frac{\mathbf{r}_1^2}{4w_{0i}^2}+\frac{\mathbf{r}_2^2}{4w_{0j}^2}\right)\right] \\ & \times \exp\left(-\frac{|\mathbf{r}_1-\mathbf{r}_2|^2}{2\delta_{ij}^2}\right)\exp[-il(\theta_1-\theta_2)] \\ & \times \exp\left[-\frac{ik}{2z}(|\boldsymbol{\rho}_1-\mathbf{r}_1|^2-|\boldsymbol{\rho}_2-\mathbf{r}_2|^2)\right] \\ & \times \langle\exp[\psi(\boldsymbol{\rho}_1,\mathbf{r}_1)+\psi^*(\boldsymbol{\rho}_2,\mathbf{r}_2)]\rangle \mathrm{d}\mathbf{r}_1\mathrm{d}\mathbf{r}_2, \end{aligned} \tag{6}$$

where k is the optical wave number related to the wavelength λ by $k = 2\pi/\lambda$. $\psi(\boldsymbol{\rho},\mathbf{r})$ stands for the random part of the complex phase of a spherical wave due to the atmospheric turbulence from the point $(\mathbf{r},0)$ to $(\boldsymbol{\rho}, z)$. The angular brackets denote averaging over the ensemble of turbulent media, which can be expressed as [31]

$$\langle\exp[\psi(\boldsymbol{\rho}_1,\mathbf{r}_1)+\psi^*(\boldsymbol{\rho}_2,\mathbf{r}_2)]\rangle = \exp\left[-\frac{1}{2}D_\psi(\boldsymbol{\rho}_1-\boldsymbol{\rho}_2,\mathbf{r}_1-\mathbf{r}_2)\right], \tag{7}$$

where $D_\psi(\boldsymbol{\rho}_1-\boldsymbol{\rho}_2,\boldsymbol{r}_1-\mathbf{r}_2)$ is the wave structure function

$$D_\psi(\boldsymbol{\rho}_1-\boldsymbol{\rho}_2,\mathbf{r}_1-\mathbf{r}_2)=8\pi^2k^2z\int_0^1\int_0^\infty\kappa\varphi_n(\kappa)\times\{1-J_0[\kappa|(1-\xi)(\boldsymbol{\rho}_1-\boldsymbol{\rho}_2)+\xi(\mathbf{r}_1-\mathbf{r}_2)|]\}\mathrm{d}\kappa\mathrm{d}\xi, \tag{8}$$

where $J_0(\kappa)$ is the first type of zero-order Bessel function and can be approximated by the first two terms. We studied the inference of the atmospheric turbulence on the polarization properties of partially coherent EGSMV beams propagating along through the horizontal path; Eq. (8) can simplified to

$$D_\psi(\boldsymbol{\rho}_1-\boldsymbol{\rho}_2,\mathbf{r}_1-\mathbf{r}_2)=\left[\frac{1}{3}\pi^2k^2z\int_0^\infty\kappa^3\varphi_n(\kappa)\mathrm{d}\kappa\right](\mathbf{r}_1-\mathbf{r}_2)^2=M(\mathbf{r}_1-\mathbf{r}_2)^2, \tag{9}$$

where $\phi_n(\kappa)$ is the atmospheric turbulence refractive index spectral density function, and we analyzed the influence of the inner and outer scales on the polarization properties through the use of the modified von Karman spectrum model, i.e.,

$$\phi_n(\kappa)=0.033C_0\exp(-\kappa^2/\kappa_m^2)(\kappa^2+\kappa_0^2)^{-11/6}, \tag{10}$$

where $\kappa_m=5.92/l_0$, $\kappa_0=2\pi/L_0$, and l_0 and L_0 represent the inner scale and outer scale, respectively. C_0 is the near-surface refractive-index structure constant of turbulent atmosphere. Substituting Eqs. (7) and (9) into Eq. (6), we obtain the following expression:

$$\begin{aligned}W_{ij}(\boldsymbol{\rho}_c,\boldsymbol{\rho}_d;z)&=A_iA_jB_{ij}\left(\frac{k}{2\pi z}\right)^2\exp\left(-\frac{ik}{z}\boldsymbol{\rho}_c\cdot\boldsymbol{\rho}_d\right)\\&\times\iint\exp\left[-\left(\frac{1}{\alpha_{ij}^2}\mathbf{r}_c^2+\frac{1}{\beta_{ij}}\mathbf{r}_c\mathbf{r}_d+\frac{1}{4\alpha_{ij}^2}\mathbf{r}_d^2\right)\right]\\&\times\exp\left(-\frac{\mathbf{r}_d^2}{2\delta_{ij}^2}\right)\exp(-il\theta_d)\exp\left(-\frac{M}{2}\mathbf{r}_d^2\right)\\&\times\exp\left[\frac{-ik}{z}(\mathbf{r}_c\cdot\mathbf{r}_d-\boldsymbol{\rho}_c\cdot\mathbf{r}_d-\boldsymbol{\rho}_d\cdot\mathbf{r}_c)\right]\mathrm{d}\mathbf{r}_c\mathrm{d}\mathbf{r}_d,\end{aligned} \tag{11}$$

where

$$\begin{cases}\mathbf{r}_c=\frac{1}{2}(\mathbf{r}_1+\mathbf{r}_2)\\\mathbf{r}_d=\mathbf{r}_1-\mathbf{r}_2\end{cases},\qquad\begin{cases}\boldsymbol{\rho}_c=\frac{1}{2}(\boldsymbol{\rho}_1+\boldsymbol{\rho}_2)\\\boldsymbol{\rho}_d=\boldsymbol{\rho}_1-\boldsymbol{\rho}_2\end{cases}, \tag{12a}$$

$$\frac{1}{\alpha_{ij}^2}=\frac{1}{4w_{0i}^2}+\frac{1}{4w_{0j}^2},\qquad\frac{1}{\beta_{ij}}=\frac{1}{4w_{0i}^2}-\frac{1}{4w_{0j}^2}. \tag{12b}$$

The variables $\mathbf{r}_c$ and $\mathbf{r}_d$ are sequentially integrated with the help of the following expansion formulas and integral formulas:

$$\int_{-\infty}^{+\infty}[e^{-ax^2}]e^{-i2\pi w_x x}\mathrm{d}x\cdot\int_{-\infty}^{+\infty}[e^{-ay^2}]e^{-i2\pi w_y y}\mathrm{d}y=\frac{\pi}{a}\cdot e^{-\frac{\pi^2w^2}{a}}, \tag{13}$$

$$\exp(-il\theta_d)=[r_{dx}-i\,\mathrm{sgn}(l)r_{dy}]^{|l|}, \tag{14}$$

$$\begin{aligned}[r_{dx}-i\,\mathrm{sgn}(l)r_{dy}]^{|l|}&=\sum_{s=0}^{|l|}\binom{|l|}{s}r_{dx}^{(|l|-s)}[-i\,\mathrm{sgn}(l)r_{dy}]^s\\&=\sum_{s=0}^{|l|}\binom{|l|}{s}[-i\,\mathrm{sgn}(l)]^s r_{dx}^{(|l|-s)}r_{dy}^s,\end{aligned} \tag{15}$$

$$\int_{-\infty}^{\infty}x^n\exp(-px^2+2qx)\mathrm{d}x=(2i)^{-n}\frac{\sqrt{\pi}}{(\sqrt{p})^{n+1}}\exp\left(\frac{q^2}{p}\right)H_n\left[i\left(\frac{q}{\sqrt{p}}\right)\right], \tag{16}$$

where $\mathrm{sgn}(\cdot)$ is a symbolic function, and $H_n(\cdot)$ denotes the Hermite polynomial of mode order n. We obtain the following expression for the CSDM of a partially coherent EGSMV beam at a pair of points with arbitrary transverse position vectors $\boldsymbol{\rho}_1=(\rho_1,\varphi_1))$ and $\boldsymbol{\rho}_2=(\rho_2,\varphi_2)$ in the receiver plane:

$$\begin{aligned}W_{ij}(\boldsymbol{\rho}_c,\boldsymbol{\rho}_d;z)&=\frac{A_iA_jB_{ij}}{\Delta_{ij}}\exp(H_{ij}\boldsymbol{\rho}_d^2+F_{ij}^2\boldsymbol{\rho}_c^2-V_{ij}\boldsymbol{\rho}_c\cdot\boldsymbol{\rho}_d)\\&\times\sum_{s=0}^{|l|}\nabla_sH_s[i(F_{ij}\boldsymbol{\rho}_{cy}-G_{ij}\boldsymbol{\rho}_{dy})]\\&\times H_{(|l|-s)}[i(F_{ij}\boldsymbol{\rho}_{cx}-G_{ij}\boldsymbol{\rho}_{dx})],\end{aligned} \tag{17}$$

where

$$C_{ij}=\frac{1}{\beta_{ij}}+\frac{ik}{z},\quad D=\frac{ik}{z},\quad E_{ij}=\frac{1}{4\alpha_{ij}^2}+\frac{1}{2\delta_{ij}^2}+\frac{M}{2}-\frac{\alpha_{ij}^2C_{ij}^2}{4}, \tag{18a}$$

$$\frac{1}{\Delta_{ij}}=\frac{k^2\alpha_{ij}^2(2i)^{-|l|}}{4z^2E_{ij}^{(|l|+2)/2}},\qquad\nabla_s=\binom{|l|}{s}[-i\,\mathrm{sgn}(l)]^s, \tag{18b}$$

$$F_{ij}=\frac{ik}{2z\sqrt{E_{ij}}},\qquad G_{ij}=\frac{\alpha_{ij}^2C_{ij}D}{4\sqrt{E_{ij}}}, \tag{18c}$$

$$H_{ij}=\frac{\alpha_{ij}^2D^2}{4}+G_{ij}^2,\qquad V_{ij}=\frac{ik}{z}\left(1+\frac{\alpha_{ij}^2C_{ij}D}{4E_{ij}}\right). \tag{18d}$$

Now let $\boldsymbol{\rho}_1=\boldsymbol{\rho}_2=\boldsymbol{\rho}$, $\boldsymbol{\rho}_c=\boldsymbol{\rho}$, $\boldsymbol{\rho}_d=0$, then the CSDM of the partially coherent EGSMV beam at a point with arbitrary transverse position vectors $\boldsymbol{\rho}=(\rho,\varphi)$ in the receiver plane can be obtained:

$$W_{ij}(\boldsymbol{\rho},\boldsymbol{\rho};z)=\frac{A_iA_jB_{ij}}{\Delta_{ij}}\exp(F_{ij}^2\boldsymbol{\rho}^2)\times\sum_{s=0}^{|l|}\nabla_sH_s[iF_{ij}\boldsymbol{\rho}_y]H_{(|l|-s)}[iF_{ij}\boldsymbol{\rho}_x]. \tag{19}$$

B. Degree of Polarization

By using the generalized Stokes parameters [32], the DoP of the partially coherent EGSMV beam propagating through atmospheric turbulence can be expressed as

$$P(\boldsymbol{\rho}; z) = \frac{\sqrt{S_1^2 + S_2^2 + S_3^2}}{S_0}, \tag{20}$$

where S_0, S_1, S_2, and S_3 are the Stokes parameters for the random beam and can be expressed by the elements of the CSDM:

$$\begin{aligned} S_0 &= W_{xx}(\boldsymbol{\rho}, \boldsymbol{\rho}; z) + W_{yy}(\boldsymbol{\rho}, \boldsymbol{\rho}; z), \\ S_1 &= W_{xx}(\boldsymbol{\rho}, \boldsymbol{\rho}; z) - W_{yy}(\boldsymbol{\rho}, \boldsymbol{\rho}; z), \\ S_2 &= W_{xy}(\boldsymbol{\rho}, \boldsymbol{\rho}; z) + W_{yx}(\boldsymbol{\rho}, \boldsymbol{\rho}; z), \\ S_3 &= i[W_{yx}(\boldsymbol{\rho}, \boldsymbol{\rho}; z) - W_{xy}(\boldsymbol{\rho}, \boldsymbol{\rho}; z)]. \end{aligned} \tag{21}$$

C. Orientation Angle of Polarization

The OAoP θ_0 ($\boldsymbol{\rho}$; z) is for the smallest angle that the major axis of the polarization ellipse makes in the x direction. Therefore, the x-, y-coordinate system is rotated in the counterclockwise sense with respect to the positive z direction, and the formula of the OAoP can be expressed as [8]

$$\theta_0(\boldsymbol{\rho}; z) = \frac{1}{2} \arctan\left\{\frac{2\,\mathrm{Re}[W_{xy}(\boldsymbol{\rho}, \boldsymbol{\rho}; z)]}{W_{xx}(\boldsymbol{\rho}, \boldsymbol{\rho}; z) - W_{yy}(\boldsymbol{\rho}, \boldsymbol{\rho}; z)}\right\}, \tag{22}$$

with $-\pi/2 \leq \theta_0 \leq \pi/2$.

3. NUMERICAL RESULTS AND ANALYSIS

Using Eqs. (19)–(21) and Eq. (22), the DoP and OAoP of a partially coherent EGSMV beam propagating through turbulent atmosphere can be calculated by simulation, which is shown as follows.

Numerical calculations are performed to illustrate the influence of source parameters and atmospheric turbulence on the DoPs and OAoPs of partially coherent EGSMV beams; some typical results are complied in Figs. 1–6. In the following numerical calculations, the calculation parameters are $B_{ij} = 0.5\exp(i\pi/4)$, $\lambda = 632.8$ nm, $\delta_{xx} = 0.02$ m, $\delta_{yy} = 0.01$ m, $\delta_{xy} = \delta_{yx} = 0.025$ m, $w_{0x} = 0.01$ m, $w_{0y} = 0.02$ m, $A_x = A_y = 1$, $l = 1$, $C_0 = 1.7 \times 10^{-14}$ m$^{-2/3}$, and $z = 1$ km, unless other values are specified in the figure captions.

Figure 1 presents the intensity distributions and DoP profiles of partially coherent EGSMV beams with different topological charges $l = 0$, $l = 1$, $l = 2$, $l = 3$, $l = 5$ in atmospheric turbulence. It is well known that the larger the topological charge is, the larger the dark spot in the center of the partially coherent EGSMV beam is, i.e., the change in intensity distribution of a partially coherent EGSMV beam is consistent with that of a general vortex beam. When the topological charge is $l = 0$, the partially coherent EGSMV beam reduces to the partially coherent EGSM beam, and its DoP increases as the off-axis distance increases and eventually approaches 1, as shown in Fig. 1(a). This result is consistent with the conclusions obtained in reference [33]. In Figs. 1(b)–1(d), we can see that when topological charges are $l = 1, 2, 3$, the DoPs of partially coherent EGSMV beams first decrease and then increase and eventually approach a certain value with the increase in off-axis distance. The DoP of the partially coherent EGSMV beam with the topological charge $l = 5$ first increases to 1 with the increase in off-axis distance, then decreases to 0, and finally increases but does not approach 1, as shown in Fig. 1(e). Comparing Figs. 1(a)–1(e), it can be found that the larger the topological charge is, the smaller the certain value that the DoP eventually approaches with increases in off-axis distance, and the more dispersed the DoP distribution of the partially coherent EGSMV beam propagating through atmospheric turbulence is. This result occurs because the larger the topological charge is, the greater the influence of the vortex beam on atmospheric turbulence is [34], and the more dispersed the DoP distribution is.

Figures 2 and 3 give the evolution of DoP profiles of partially coherent EGSMV beams with topological charge $l = 1$ propagating in atmospheric turbulence for different wavelengths and near-surface refractive index structure constants. Figures 2 and 3 show that the longer the wavelength and the smaller the near-surface refractive index structure constant are, the more concentrated the DoP distribution of the partially coherent EGSMV beam propagating in atmospheric turbulence is. However, no matter how the wavelength and the near-surface refractive index structure constant change, the DoP of the partially coherent EGSMV beam first decreases and then increases with the increase in off-axis distance, and eventually approaches a certain value. This certain value decreases with the increase in the wavelength, but it is always 1 regardless of how the near-surface refractive index structure constant changes. In addition, it is found that the longer the wavelength and the smaller the near-surface refractive index structure constant are, the larger the on-axis DoP of the partially coherent EGSMV beam propagating in atmospheric turbulence is. This result occurs because the smaller the near-surface refractive index structure constant is, the weaker the atmospheric turbulence is and the less the influence of atmospheric turbulence on the partially coherent EGSMV beam is.

Figure 4 gives the evolution of DoP profiles of the partially coherent EGSMV beam with topological charge $l = 1$ propagating through atmospheric turbulence for different inner and outer scales. For the same outer scale, the larger the inner scale is, the more concentrated the DoP distribution and the larger the on-axis DoP of the partially coherent EGSMV beam propagating in atmospheric turbulence are. In the case of different outer scales, the DoP profiles are very close. It can be seen that the outer scale is negligible for analyzing the influence of atmospheric turbulence on the polarization properties of partially coherent EGSMV beams. This result is similar to that of the Gaussian beam. The main physical reason for this result is that the smaller the inner scale is, the smaller the turbulent vortices on the cross section of the beam are and the more severe the diffraction of the beam is. Therefore, the beam is more randomly distributed in space and time, and the DoP distribution is more dispersed. In addition, no matter how the inner and outer scales change, the DoP of the partially coherent EGSMV beam first decreases and then increases with the increase in off-axis distance, and eventually approaches 1.

Figure 5 gives the variation of DoP distributions and on-axis point DoPs of partially coherent EGSMV beams propagating in atmospheric turbulence with the propagation distance under different topological charges of $l = 0, 1, 2, 3, 4, 5$. It can be seen in Figs. 5(a)–5(f) that the DoP tends toward a constant value with the increase in propagation distance, and as the topological charge increases, this constant value decreases first

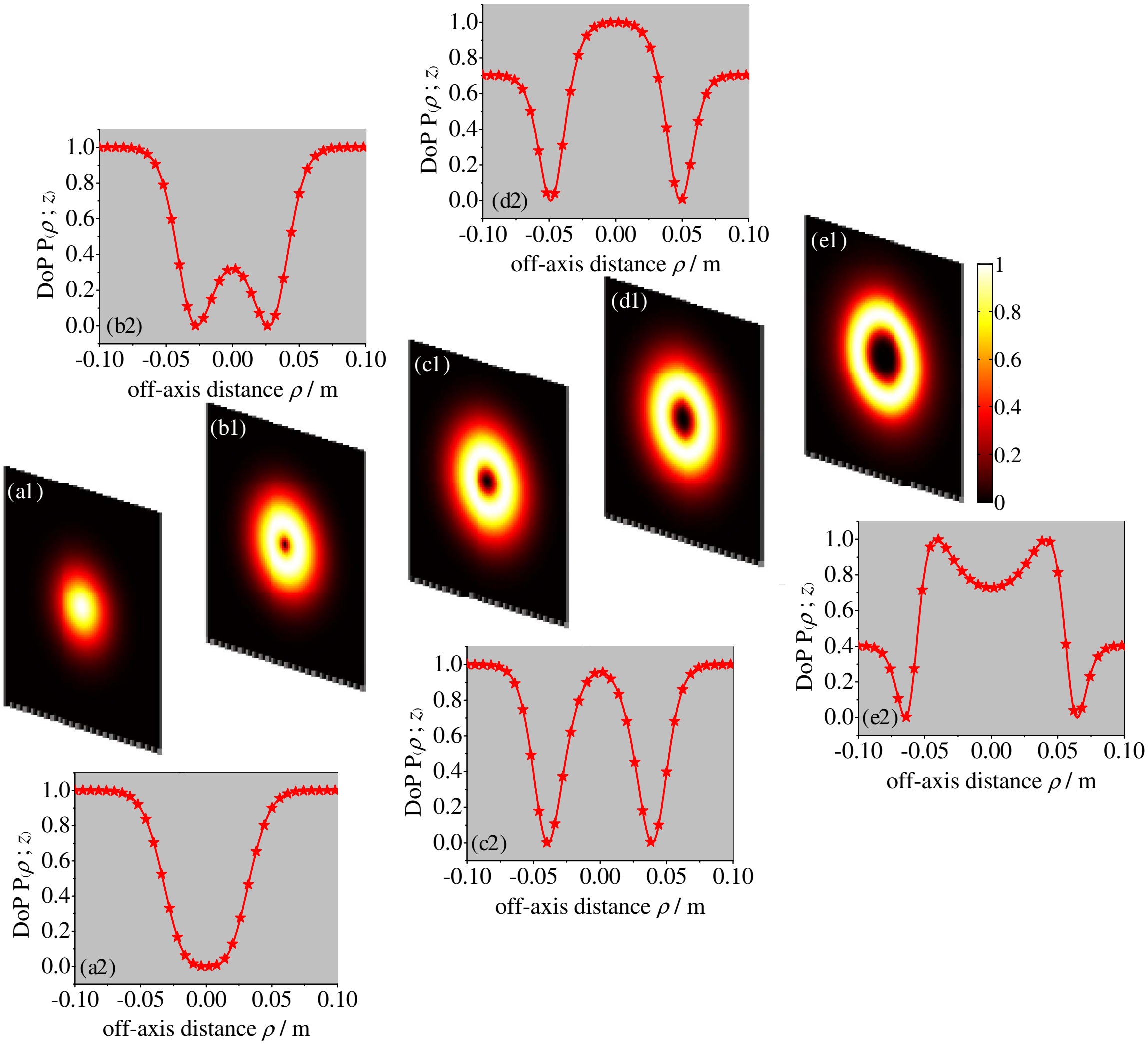

Fig. 1. DoP profiles and intensity distributions of partially coherent EGSMV beams with different topological charges in atmospheric turbulence: (a) $l = 0$; (b) $l = 1$; (c) $l = 2$; (d) $l = 3$; (e) $l = 5$.

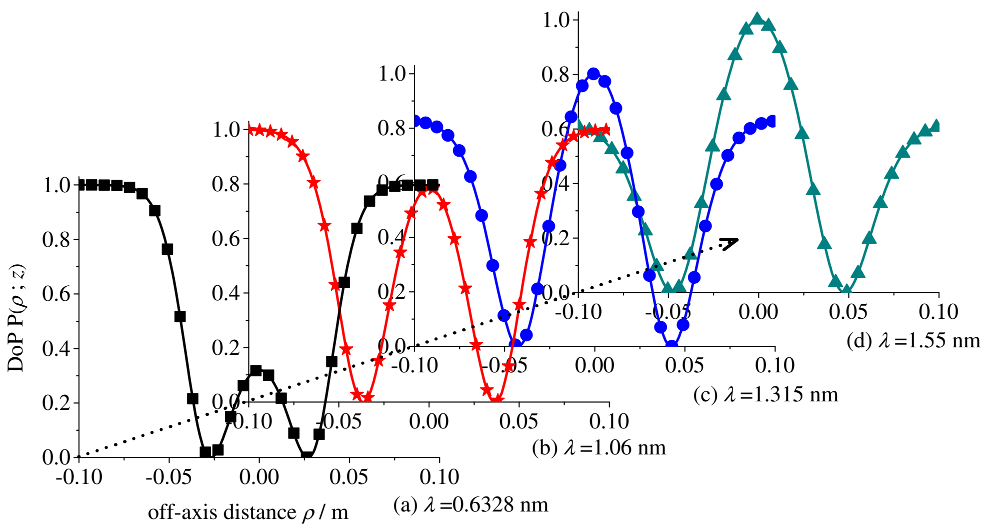

Fig. 2. Evolution of DoP profiles of partially coherent EGSMV beams with topological charge $l = 1$ in atmospheric turbulence for different wavelengths.

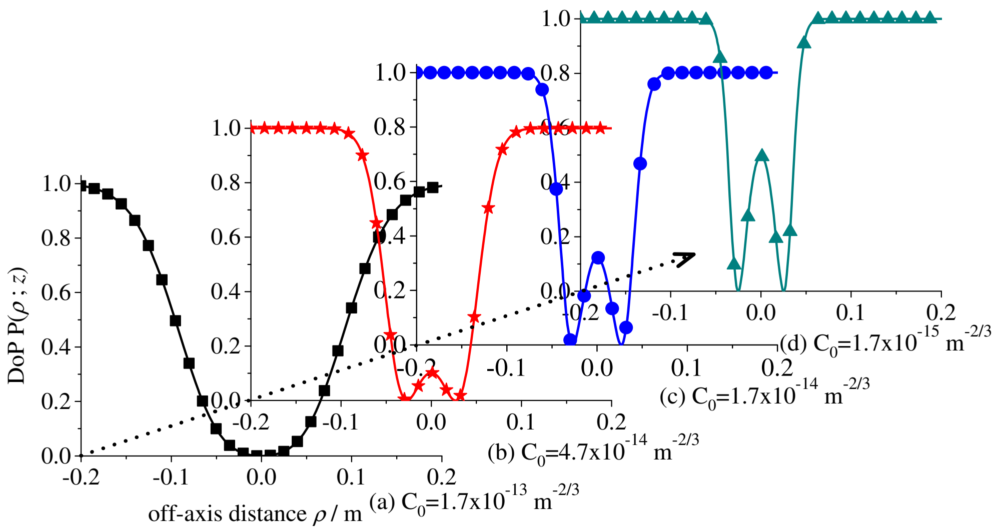

Fig. 3. Evolution of DoP profiles of partially coherent EGSMV beams with topological charge $l = 1$ in atmospheric turbulence for different near-surface refractive index structure constants.

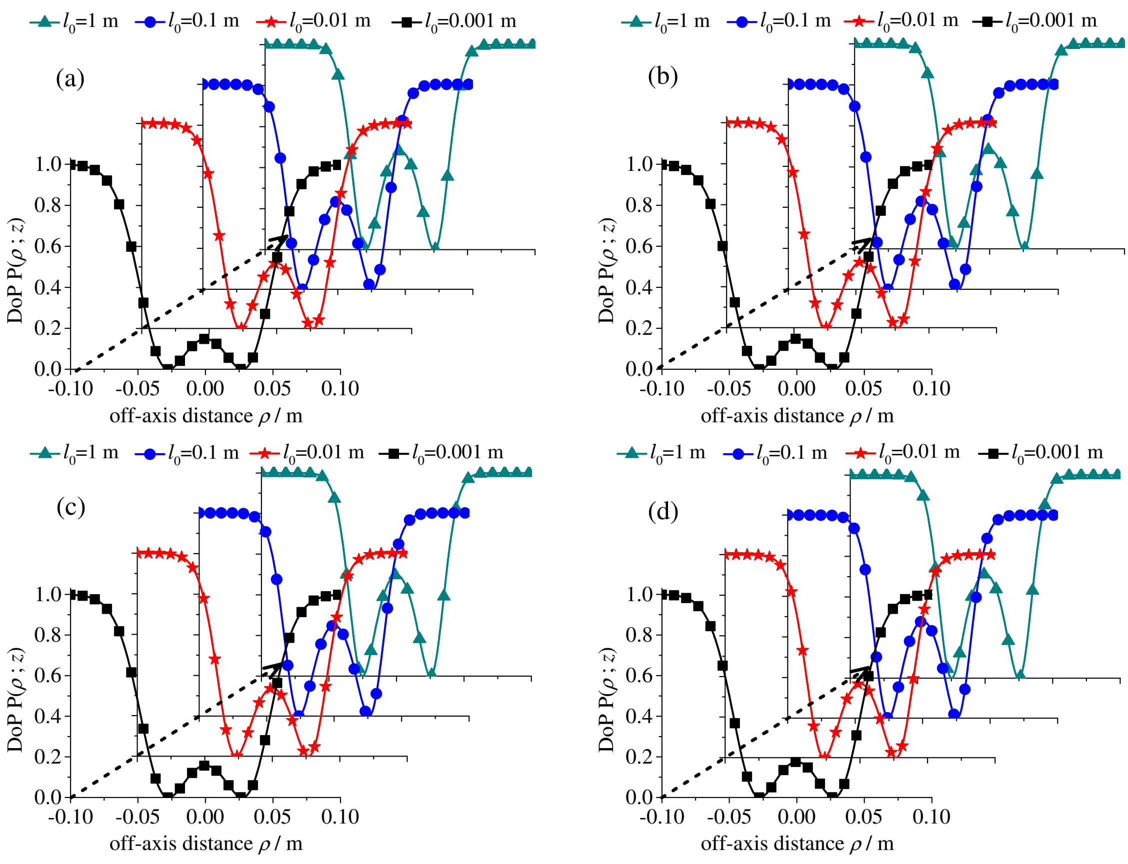

Fig. 4. Evolution of DoP profiles of partially coherent EGSMV beams with topological charge $l = 1$ in atmospheric turbulence for different inner and outer scales: (a) $L_0 = 200$ m; (b) $L_0 = 100$ m; (c) $L_0 = 10$ m; (d) $L_0 = 1$ m.

and then increases. When the topological charge is 0 (i.e., the partially coherent EGSMV beam reduces to the partially coherent EGSM beam), with the increase in propagation distance, the on-axis point DoP gradually increases to a constant value. When the topological charge is greater than 0 (i.e., the partially coherent EGSMV beam carries vortex information), the on-axis point DoP eventually shows a decreasing trend as propagation distance increases. With the combined

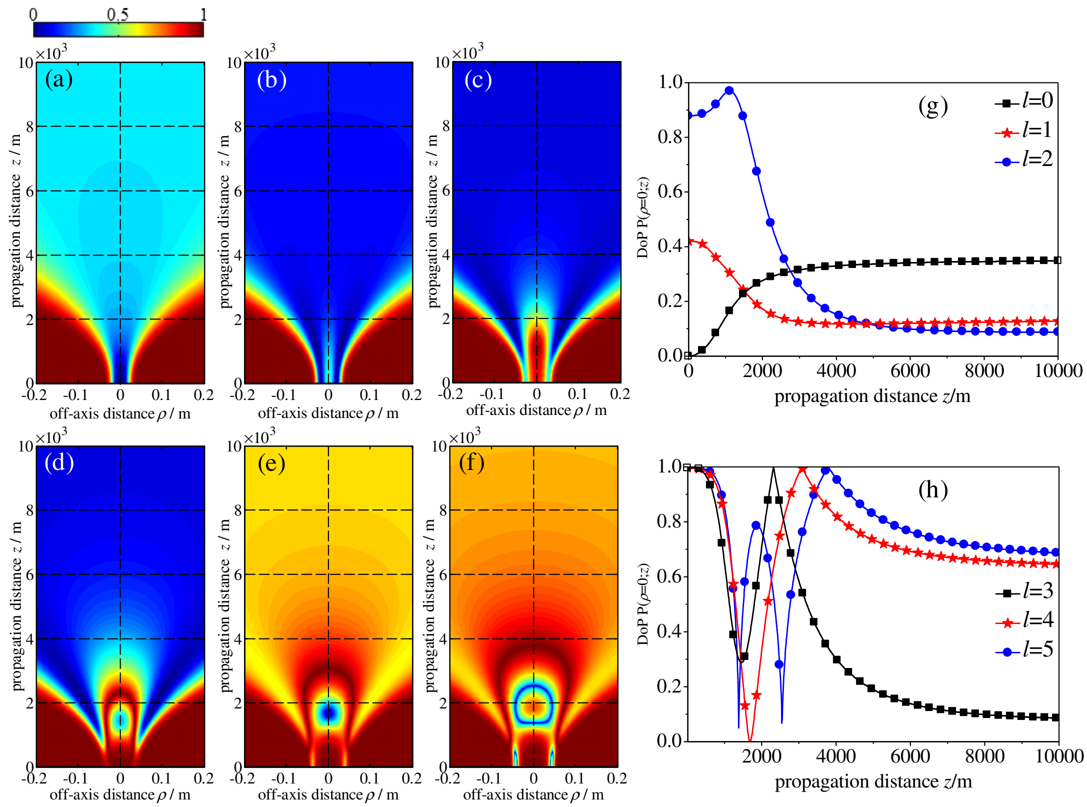

Fig. 5. (a)–(f) DoP distributions and (g), (h) on-axis point DoPs of partially coherent EGSMV beams with different topological charges with the change in propagation distance: (a) $l = 0$; (b) $l = 1$; (c) $l = 2$; (d) $l = 3$; (e) $l = 4$; (f) $l = 5$.

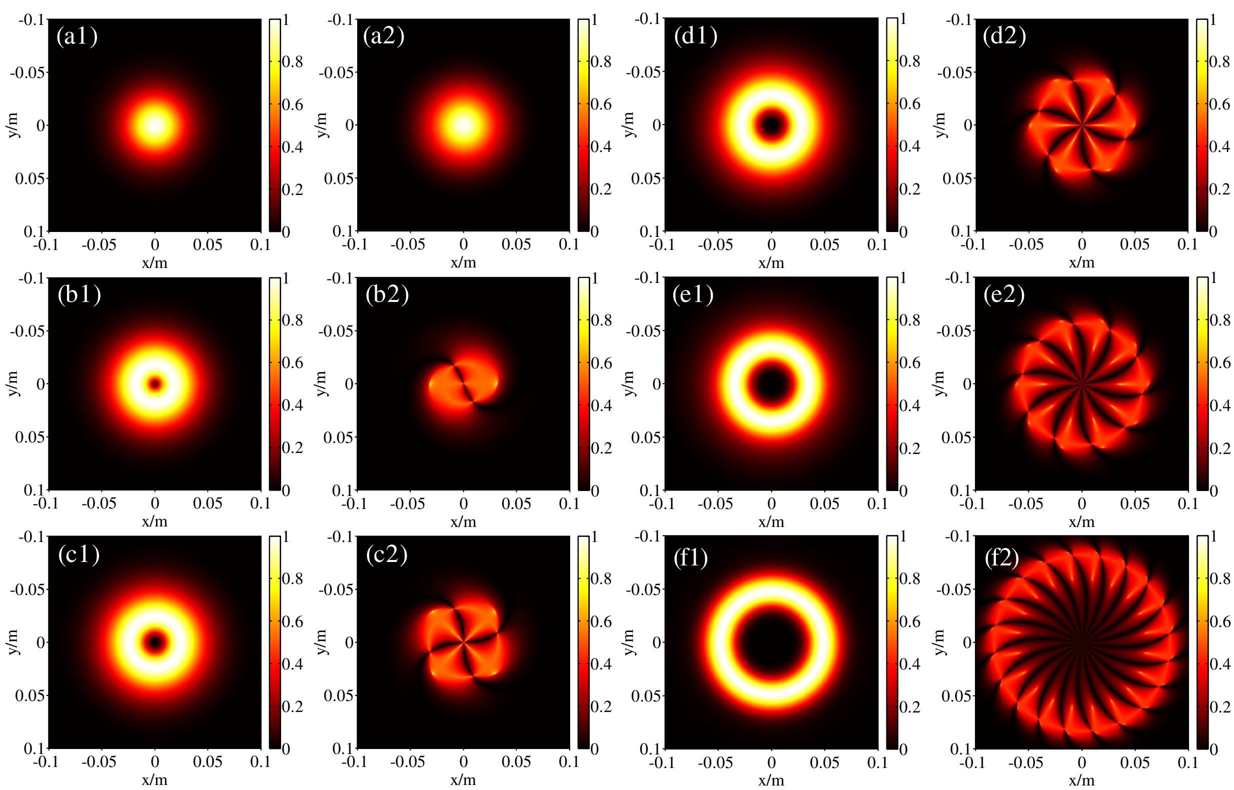

Fig. 6. Intensity distributions (a1)–(f1) and OAoP distributions (a2)–(f2) of partially coherent EGSMV beams with different topological charges: (a) $l = 0$; (b) $l = 1$; (c) $l = 2$; (d) $l = 3$; (e) $l = 5$; (f) $l = 10$.

Figs. 5(g) and 5(f), we can see that the larger the topological charge is, the larger the initial DoP of the partially coherent EGSMV beam is. As propagation distance increases, the oscillation of the DoP becomes more and more severe, but the larger the topological charge is, the propagation distance corresponding to the DoP reaching a constant value also increases. This also shows that the larger the topological charge, the more the information that can be received by the detector when the partially coherent EGSMV beam propagates in atmospheric turbulence.

Figure 6 gives the intensity and OAoP distributions of partially coherent EGSMV beams with topological charges of $l = 0$, $l = 1$, $l = 2$, $l = 3$, $l = 5$, $l = 10$ propagating in atmospheric turbulence. Figures 6(a1)–6(f1) present the intensity distributions of partially coherent EGSMV beams for different topological charges. As shown in Figs. 6(a1)–6(f1), with the increase in the number of the topological charge, the dark spot of the intensity distribution of the partially coherent electromagnetic vortex beam increases gradually. This feature was well established in previous studies. As can also be seen in Figs. 6(a2)–6(f2), the larger the topological charge is, the wider the OAoP distribution of the partially coherent EGSMV beam is. When the topological charge is 0 (i.e., the partially coherent EGSMV beam reduces to the partially coherent EGSM beam), the OAoP distribution of the partially coherent EGSMV beam is Gaussian-like distribution. When the topological charge is greater than 0 (i.e., the partially coherent EGSMV beam carries vortex information), the OAoP distribution of the partially coherent EGSMV beam is in the shape of a petal. We can also find in Figs. 6(a2)–6(f2) that the number of petals is related to the topological charge, which is equal to twice the topological charge of the partially coherent EGSMV beam. Therefore, we can measure the topological charge l according to the OAoP distribution of the partially coherent EGSMV beam.

4. CONCLUSION

In conclusion, the polarization properties of partially coherent EGSMV beams have been studied. We analyzed the influence of factors such as topological charge, wavelength, propagation distance, near-surface refractive index structure constant, and inner and outer scales on the polarization properties of partially coherent EGSMV beams. Based on numerical simulation, we can draw new conclusions: (1) the larger the topological charge is, the larger the dark spot in the center of the partially coherent EGSMV beam, the more dispersed the DoP distribution, and the wider the OAoP distribution are; (2) the longer the wavelength and the smaller the near-surface refractive index structure constant are, the more concentrated the DoP distribution is; (3) the larger the inner scale is, the more concentrated the DoP distribution is, but the outer scale is negligible for analyzing the influence of atmospheric turbulence on the polarization properties of partially coherent EGSMV beams; (4) the number of petals, which is the shape of the OAoP distribution, is equal to just twice the topological charge of the partially coherent EGSMV beam. These results provide a theoretical basis for better control of coherent detection in optical communication when the partially coherent EGSMV beam propagating through atmospheric turbulence is used as the local oscillator in the wireless optical communication system.

Funding. Key Industrial Innovation Chain Project of Shaanxi Province (2017ZDCXL-GY-06-01); National Natural Science Foundation of China (NSFC) (61771385); Xi'an Science and Technology Planning Project (2017080CG/RC043(XALG015), 201805037YD15CG21(9)); Natural Science Basic Research Program (2018JQ6032).

REFERENCES

1. J. L. Alvarez-Perez, "Coherence polarization and statistical independence in Cloude-Pottier's radar polarimetry," IEEE T. Geosci. Remote **49**, 426–441 (2011).
2. C. J. Yu and C. M. Hsieh, "Electrically controllable polarization element," IEEE Photon. Technol. Lett. **28**, 1229–1232 (2016).
3. X. Tang, Z. Ghassemlooy, S. Rajbhandari, W. O. Popoola, and C. G. Lee, "Coherent heterodyne multilevel polarization shift keying with spatial diversity in a free-space optical turbulence channel," J. Lightwave Technol. **30**, 2689–2695 (2012).
4. J. Wu, "Propagation of a Gaussian-Schell beam through turbulent media," J. Mod. Opt. **37**, 671–684 (1990).
5. J. Wu and A. D. Boardman, "Coherence length of a Gaussian-Schell beam and atmospheric turbulence," J. Mod. Opt. **38**, 1355–1363 (1991).
6. M. Salem, O. Korotkova, A. Dogariu, and E. Wolf, "Polarization changes in partially coherent electromagnetic beams propagating through turbulent atmosphere," Waves Random Media **14**, 513–523 (2014).
7. E. Wolf, "Unified theory of coherence and polarization of random electromagnetic beams," Phys. Lett. A **312**, 263–267 (2003).
8. O. Korotkova and E. Wolf, "Changes in the state of polarization of a random electromagnetic beam on propagation," Opt. Commun. **246**, 35–43 (2005).
9. H. T. Eyyuboglu, Y. Baykal, and Y. Cai, "Degree of polarization for partially coherent general beams in turbulent atmosphere," Appl. Phys. B **89**, 91–97 (2007).
10. H. Lin and J. Pu, "Propagation properties of partially coherent radially polarized beam in a turbulent atmosphere," J. Mod. Opt. **56**, 1296–1303 (2009).
11. G. Zheng, L. Wang, J. Wang, M. Zhou, and M. Song, "Propagation properties of a partially coherent radially polarized beam in atmospheric turbulence," J. Mod. Opt. **65**, 1616–1621 (2018).
12. G. Basso, I. Vidal, and L. Oliveira, "Complete characterization of partially coherent and partially polarized optical fields," Opt. Lett. **39**, 1220–1222 (2014).
13. L. Allen, M. W. Beijersbergen, R. J. C. Spreeuw, and J. P. Woerdman, "Orbital angular momentum of light and the transformation of Laguerre-Gaussian laser modes," Phys. Rev. A **45**, 8185–8189 (1992).
14. Z. Liu and D. Zhao, "Spectral density of vortex beams propagating in atmospheric turbulence with new simulation method," Opt. Lett. **43**, 2478–2481 (2018).
15. G. Gbur and R. K. Tyson, "Vortex beam propagation through atmospheric turbulence and topological charge conservation," J. Opt. Soc. Am. A **25**, 225–230 (2008).
16. J. Ou, Y. Jiang, and Y. He, "Intensity and polarization properties of elliptically polarized vortex beams in turbulent atmosphere," Opt. Laser Technol. **67**, 1–7 (2015).
17. M. Luo and D. Zhao, "Determining the topological charge of stochastic electromagnetic vortex beams with the degree of cross-polarization," Opt. Lett. **39**, 5070–5073 (2014).
18. H. Li, F. Honary, J. Wang, J. Liu, Z. Wu, and L. Bai, "Intensity, phase, and polarization of a vector Bessel vortex beam through multilayered isotropic media," Appl. Opt. **57**, 1967–1976 (2018).
19. Y. Kozawa and S. Sato, "Focusing of higher-order radially polarized Laguerre-Gaussian beam," J. Opt. Soc. Am. A **29**, 2439–2443 (2012).

20. J. Wang, L. Wang, Y. Xin, and M. Song, "Polarization properties of superposed vector Laguerre-Gaussian beams during propagation," J. Opt. Soc. Am. A **34**, 1924–1933 (2017).
21. S. Vyas, Y. Kozawa, and S. Sato, "Polarization singularities in superposition of vector beams," Opt. Express **21**, 8972–8986 (2013).
22. S. Vyas, Y. Kozawa, and Y. Miyamoto, "Creation of polarization gradients from superposition of counter propagating vector LG beams," Opt. Express **23**, 33970–33979 (2015).
23. M. Tang, D. Zhao, X. Li, and H. Li, "Focusing properties of radially polarized multi-cosine Gaussian correlated Schell-model beams," Opt. Commun. **396**, 249–256 (2017).
24. M. Tang, D. Zhao, X. Li, and J. Wang, "Propagation of radially polarized multi-cosine Gaussian Schell-model beams in non-Kolmogorov turbulence," Opt. Commun. **407**, 392–397 (2018).
25. K. Huang, P. Shi, G. W. Cao, K. Li, X. B. Zhang, and Y. P. Li, "Vector-vortex Bessel-Gauss beams and their tightly focusing properties," Opt. Lett. **36**, 888–890 (2011).
26. X. Liu and J. Pu, "Investigation on the scintillation reduction of elliptical vortex beams propagating in atmospheric turbulence," Opt. Express **19**, 26444–26450 (2011).
27. D. Liu, Y. Wang, and H. Yin, "Propagation properties of partially coherent four-petal Gaussian vortex beams in turbulent atmosphere," Opt. Laser Technol. **78**, 95–100 (2016).
28. K. Wu, Y. Huai, T. Zhao, and Y. Jin, "Propagation of partially coherent four-petal elliptic Gaussian vortex beams in atmospheric turbulence," Opt. Express **26**, 30061–30075 (2018).
29. X. Zhao, Y. Yao, Y. Sun, and C. Liu, "Condition for Gaussian Schell-model beam to maintain the state of polarization on the propagation in free space," Opt. Express **17**, 17888–17894 (2009).
30. O. Korotkova, M. Salem, and E. Wolf, "The far-zone behavior of the degree of polarization of electromagnetic beams propagating through atmospheric turbulence," Opt. Commun. **233**, 225–230 (2004).
31. S. C. H. Wang and M. A. Plonus, "Optical beam propagation for a partially coherent source in the turbulent atmosphere," J. Opt. Soc. Am. **69**, 1297–1304 (1979).
32. O. Korotkova and E. Wolf, "Generalized Stokes parameters of random electromagnetic beams," Opt. Lett. **30**, 198–200 (2005).
33. X. Z. Ke and J. Wang, "Comparison of polarization property of partially coherent beam between propagating along an uplink path and a downlink path in atmospheric turbulence," Acta Phys. Sin. **64**, 224204 (2015).
34. F. Li, "Propagation characteristics of optical vortices beam in intermediate fluctuation turbulent atmosphere," Laser Optoelectron. Prog. **50**, 070101 (2013).